

## Electrochemical sensor based on poly (aspartic acid) modified carbon paste electrode for paracetamol determination

Mohammed Monirul Islam<sup>1,\*</sup>, MD Arifuzzaman<sup>2</sup>, Sayeed Rushd<sup>3</sup>, MD Kamrul Islam<sup>4</sup>, and Muhammad Muhitur Rahman<sup>5</sup>

<sup>1</sup> Department of Biomedical Sciences, College of Clinical Pharmacy, King Faisal University, Al-Ahsa, 31982, Saudi Arabia

<sup>2</sup> Department of Civil and Environmental Engineering, College of Engineering, King Faisal University, Al-Ahsa, 31982, Saudi Arabia

<sup>3</sup> Department of Chemical Engineering, College of Engineering, King Faisal University, Al-Ahsa, 31982, Saudi Arabia

<sup>4</sup> Department of Civil and Environmental Engineering, College of Engineering, King Faisal University, Al-Ahsa, 31982, Saudi Arabia

<sup>5</sup> Department of Civil and Environmental Engineering, College of Engineering, King Faisal University, Al-Ahsa, 31982, Saudi Arabia

\*E-mail: [mislam@kfu.edu.sa](mailto:mislam@kfu.edu.sa)

Received: 3 November 2021 / Accepted: 15 December 2021 / Published: 5 January 2022

---

Electrocatalytic determination of paracetamol (PRT) in presence of cetirizine (CN) at the carbon paste sensor (CPS) modified with poly aspartic acid (PA) via electrochemical polymerization method was discussed. Oxidation of PRT at the poly (aspartic acid) modified carbon paste sensor (PAMCPS) followed at low overpotential and voltammetric information showed that it was an absolutely surface controlled response involving equal number of electrons and protons transfer. The modified sensor displays great catalytic activity for the oxidation of PRT with great sensitivity over the concentration range of 10.0  $\mu\text{M}$  to 105.0  $\mu\text{M}$ , with the detection limit (DL) of 53.37 nM ( $S/N = 3$ ) and quantification limit (QL) of 117.93 nM ( $S/N=10$ ). Characterization of the sensor materials were done using field emission scanning electron microscopy (FE-SEM) and cyclic voltammetry (CV). Electrochemical investigations revealed that the proposed sensor displayed some significant benefits, including high effective surface area, numerous reactive sites and excellent electrochemical catalytic activity toward the oxidation and reduction of PRT. This sensor showed an excellent stability, selectivity, sensitivity, reproducibility and repeatability, recommending that the sensor was a promising one for the simultaneous determination of PRT and CN in real sample with acceptable recovery.

---

**Keywords:** Cetirizine; Paracetamol; Carbon paste electrode; Polymerization; Electroanalysis.

## 1. INTRODUCTION

Electrochemical strategies offer helpful option since they permit a quicker and exact investigation [1, 2]. Electrochemical assurance of PRT is either by reduction or oxidation. Oxidation of PRT offers a few benefits, to be specific no obstruction from PRT molecules. The utilization of unmodified electrodes like carbon electrodes, platinum electrodes and gold electrodes for the oxidation of PRT shows very weak peak. A decent method for the determination of PRT by utilizing modified electrodes. One of the main impacts of any modifier is a decrease of the overpotential needed for the electrochemical response and improvement of the sensitivity and selectivity of the technique. The turn of events and use of polymer modified electrodes have gotten significant consideration as of late because of their many benefits, like simple method of preparation, non-poison, low cost, wider operational potential window, sustainable surface, stability in different solvents and longer life time [3,4]. The modifying of electroactive materials into a sensor is beneficial and has been broadly applied in the electroanalytical research area. The fabrication of the sensor surface with polymer films is subsequently a promising methodology for working on the force and scope of electrochemically fabricated sensors. This new class of sensor material has been found helpful to improve the sensor sensitivity and selectivity and to decrease fouling impacts in numerous applications in particular for PRT oxidation. The electro polymerization offers the renewable modification as far as thickness and film stacking. Paracetamol is a typical painkiller used to treat hurts and torment. It can likewise be utilized to diminish a high temperature [5,6]. Accordingly, the identification of paracetamol is fundamental and has acquired broad consideration among the scientists around the world. To consider the paracetamol in biological samples, and to monitor the therapeutic concentration of its compound, it is important to foster profoundly sensitive and specific analytical strategies fit for determining the paracetamol [7, 8]. PRT is generally utilized for remedial applications, its determination and quality control assume critical part. A few scientific techniques have been generally utilized for the separation and evaluation of paracetamol in biological samples, including capillary electrophoresis [9], high performance liquid chromatography (HPLC) [10], spectrophotometry [11], flow injection [12] and various advanced voltammetric techniques [13–25]. With the exception of voltammetric strategies the other old-style techniques have few drawbacks like monotonous example pre-treatment before investigation, extensive and tedious strategy, low sensitivity and high instrument cost [26-36]. In the current work, we have electrode modified by utilizing a polymerization method with Aspartic acid. Tests were directed for the determination of PRT and cetirizine utilizing a PAMCPS. The fabricated sensor has been utilized for the voltammetric recognition of PRT, which shows the better electrocatalytic action towards the determination of the PRT as compare unmodified carbon paste electrode.

## 2. EXPERIMENTAL

### 2.1 Materials and reagents

Paracetamol, Cetirizine, and silicone oil were taken from Sigma-Aldrich. Graphite, monobasic phosphate ( $\text{NaH}_2\text{PO}_4$ ) and dibasic phosphate ( $\text{Na}_2\text{HPO}_4$ ) were taken from Merck and all the reagents were used without purification. All the solutions were prepared with ultra-purified water.

## 2.2 Instruments

CV and DPV are conducted using electrochemical device. The electrochemical cell was instituted for this effort involves three-electrodes such as, PAMCPS and BCPS as a working electrode, Hg<sub>2</sub>Cl<sub>2</sub> saturated with KCl is a reference electrode, and a Pt wire is counter electrode. This complete investigation was finished at the temperature of (25±2) °C.

## 2.3 Preparation of electrodes

The BCPS was accomplished via the mixing of silicon oil and graphite powder having 70:30 of weight percentage ratio up to the identical graphite paste was achieved. The achieved identical paste was packed in to the hole (3.0 mm of diameter) of Teflon tube and its peripheral was levelled by rubbing on a soft paper. The electrical support was permitted through a copper tip connected to the graphite paste. The PAMCPS was prepared by means of the elector-polymerization process. The electro-polymerization of 1.0 mM aspartic acid in 0.2 M PBS of 7.0 pH at CPS was done by means of 10.0 CV cycles with the potential slit of -0.1 to 1.5 V at 0.1 V/s scan rate. Then, the prepared electrodes were carefully rinsed with distilled water to remove the materially adsorbed contaminations [16].

## 3. RESULTS AND DISCUSSION

### 3.1 FE-SEM characterization of the fabricated sensor

The morphology examination of the surface of the modified electrode were considered by FE-SEM technique (Fig. 1). The FE-SEM pictures showed a uniform surface framed with the various compounds of the modified electrode (graphite, silicone oil and polymer). Polymer film was homogeneously distributed on the graphite in the presence of silicone oil as a binder.

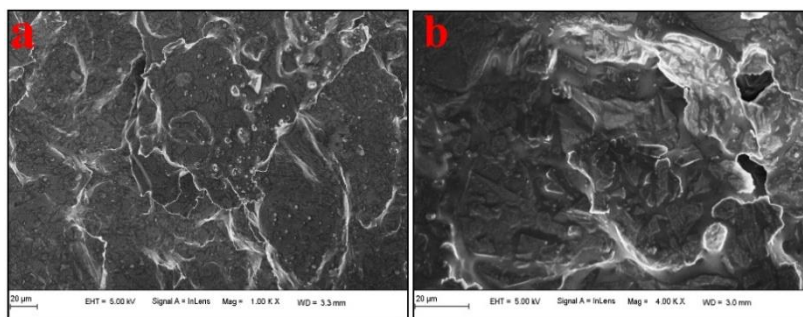


**Figure 1.** FE-SEM images of a: BCPS and b: PAMCPS.

### 3.2 Analysis of surface area

At first, the standard 1.0 mM K<sub>4</sub>[Fe(CN)<sub>6</sub>] in 0.1 M KCl was subjected to CV at modified and unmodified sensors for the analysis the electrochemical surface area. Fig. 2 shows the documented cyclic

voltammograms for  $K_4[Fe(CN)_6]$  in KCl at BCPS and PAMCPS. Observations reveals that, the modified sensor (PAMCPS) displays high electrochemical peak response than the unmodified sensor (BCPS). The surface area of BCPS and PAMCPS was premeditated through the usage of the following Randles-Sevcik's equation [37, 38],

$$I_p = 2.69 \times 10^5 n^{3/2} A D^{1/2} v^{1/2} C_0 \quad (Eqn. 1)$$

where, A is the operational surface area of the sensor, n is the number of electrons involved in the redox reaction of  $K_4[Fe(CN)_6]$ , D is the diffusion coefficient of  $K_4[Fe(CN)_6]$ ,  $C_0$  is the concentration of  $K_4[Fe(CN)_6]$  and v is the scan rate. The calculated operational surface area for BCPS, and PAMCPS are achieved to be  $0.0184 \text{ cm}^2$  and  $0.043 \text{ cm}^2$ , individually. The achieved outcome indicates that the superior surface area of modified electrode is due to the strong interaction between poly (aspartic acid) and CPS surface.

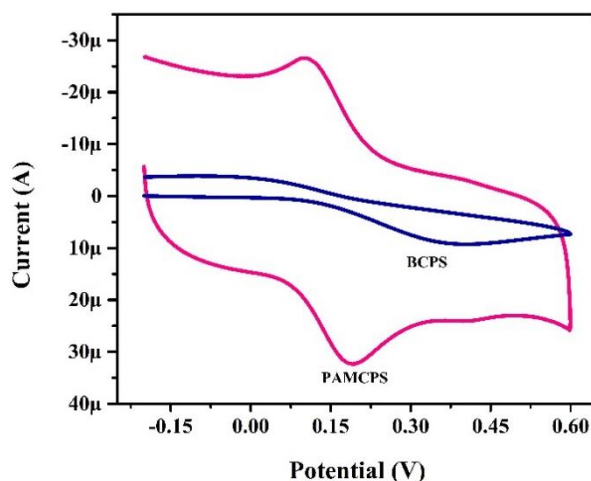


**Figure 2.** CVs for 1.0 mM  $K_4[Fe(CN)_6]$  in 0.1 M KCl solution on BCPS and PAMCPS at 0.1 V/s of scan rate.

### 3.3 Electro-polymerization of aspartic acid on CPS surface

The development of poly (aspartic acid) on CPS was attained by means of the electro-polymerization method. The ten CV cycles were operated for 1.0 mM aspartic acid in 0.2 M PBS of 7.0 pH at CPS with the potential slit of -0.1 to 1.5 V at 0.1 V/s scan rate. Fig. 3 shows the regularly enhanced cyclic voltammograms (based on peak current), which consents the alteration of aspartic acid into poly (aspartic acid) on CPS. The attained poly (aspartic acid) layer has a robust connection with CPS surface through covalent bonding among Carbon and Nitrogen.

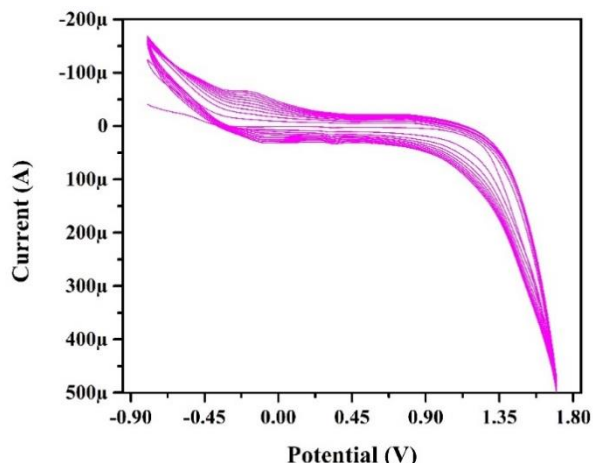


**Figure 3.** CVs for 1.0 mM aspartic acid in 0.2 M PBS of 7.0 pH on CPS at 0.1 V/s of scan rate and -0.1 to 1.5 V of potential window.

### 3.2 Electrochemical behavior of PRT at BCPS and PAMCPS

The redox behavior of 0.1mM PRT at BCPS and PAMCPS was examined in pH 7.0 PBS to discuss about their peak improvement impact. Fig. 4 shows the cyclic voltammograms for 0.1 mM PRT at BCPS and PAMCPS in 0.1 M PBS with pH 7.0 at the scan rate of 0.1 Vs<sup>-1</sup>. At BCPS, the redox peak of PRT was not clear with low current response and high peak potential. But, under identical conditions PAMCPS showed huge improvement in the current response with reduced peak potential. The improvement in the peak current of PRT at PAMCPS might be attributed to few potential reasons, this can be attributed to high conductivity and good electron transportation properties of PAMCPS. Nevertheless, in blank solution no peak is observed at PAMCPS. Based on these perceptions, it tends to be proposed that the PAMCPS shows a powerful heterogeneous electro-catalyst in the electrochemical reaction of PRT, prompting a momentous improvement of the anodic and cathodic peak current. Also,  $I_{pa}/I_{pc}$  was not equal to the theoretical value of 1.0, hence the reaction nature of PRT is a quasi-reversible at PAMCPS (18).

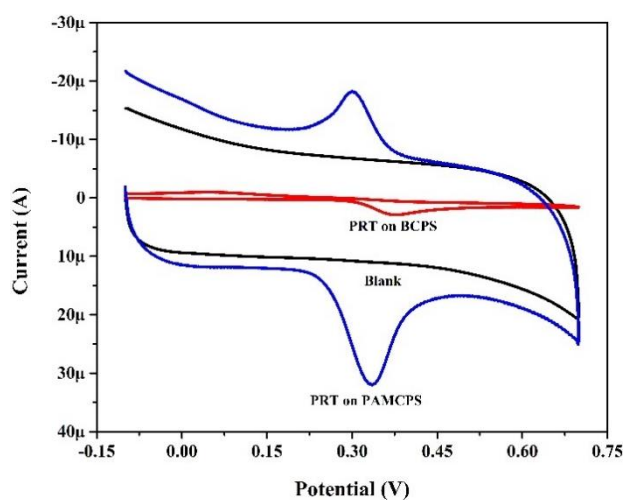


**Figure 4.** CVs for the presence and absence (blank) of 0.1 mM PRT in 0.2 M PBS of 7.0 pH on BCPS and PAMCPS at 0.1 V/s of scan rate.

### 3.2 The effect of scan rate

The impact of the scan rate (from 0.1 to 0.25 V/s) on the electrochemical reaction was explored for a 0.1 mM PRT in a 0.1 M PBS (pH 7.0) by utilizing the PAMCPS. As can be found in Fig. 5a, there was a shift in the oxidation peak potential to more negative values as the scan rate increased. Additionally, Fig. 5b indicates the relation among log  $I_{pa}$  vs log  $v$ , which shows a decent linear arrangement with the linear regression equality is shown as follows,

$$\log I_{pa} (\mu A) = 3.748 + 0.790 \log v (V/s) \quad (R = 0.998) \quad (\text{Eqn. 2})$$

The attained slope of 0.790 recommends that, the catalytic action of PAMCPS for the oxidation nature of PRT was accomplished by adsorption-controlled process [39]. Supporting to this, a linear relationship between the oxidation peak current and the scan rate was obtained with fine linearity and the relation is as follows (Fig. 5c),

$$I_{pa} (\mu A) = 1.088 \times 10^{-4} + 2.085 \times 10^{-4} v (V/s) \quad (R = 0.998) \quad (\text{Eqn. 3})$$

Here the regression coefficient (R) value is very near to theoretical value and suggests that the PRT oxidation reaction is adsorption-controlled [40].

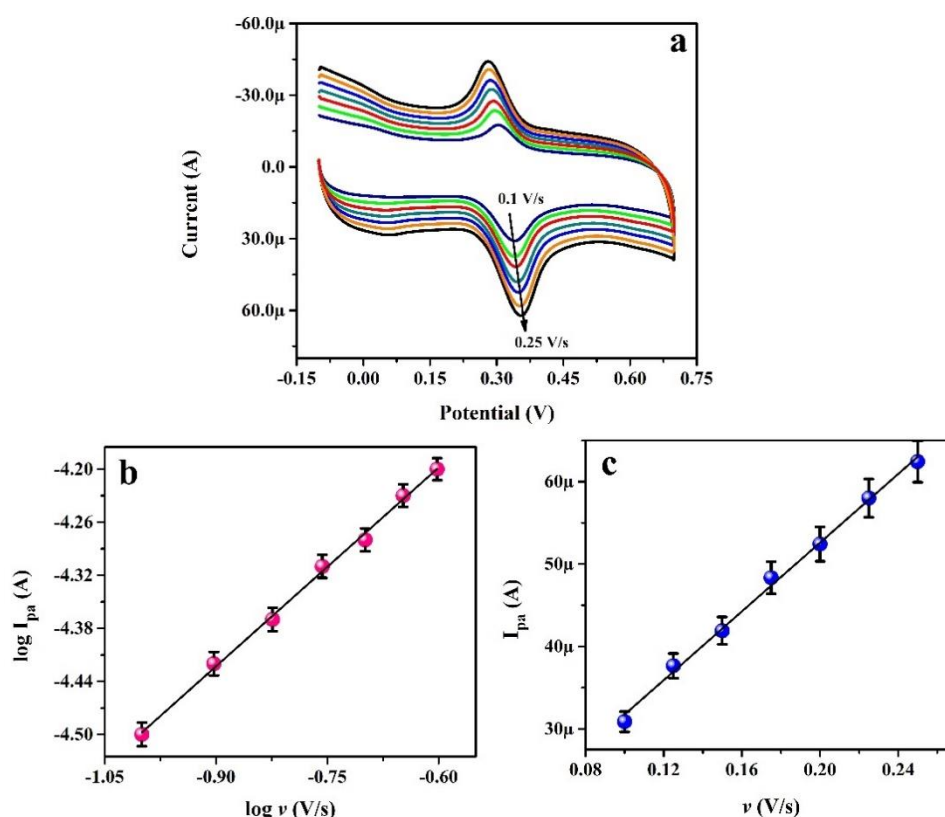


**Figure 5.** (a) CVs of 0.1 mM PRT in 0.2 M PBS of 7.0 pH on PAMCPS at different scan rate from 0.1 – 0.25 V/s. (b) Plot of log  $I_{pa}$  vs log  $v$ . (c) Plot of  $I_{pa}$  vs  $v$ .

### 3.2 The pH effect

The impact of pH of the supporting electrolyte was likewise examined by changing the pH in the range 5.5–8.0 (Fig. 6). The influence of pH on the peak current and the peak potential for the oxidation of PRT is clearly found in Fig. 6a as insets. The anodic peak potentials shifted negatively and widened as the pH increases (Fig. 6b), revealing that the electrocatalytic oxidation of PRT was a pH-dependent (slope=-0.713) response with participation of protons and that the proton-transfer reaction precedes the electron transfer, i.e., two electrons transferred per molecule. As can be seen from Fig. 6c, the peak current of the PRT increases as the escalation of pH 5.5 to pH 8.0. At pH 7.0, the peak current is maximum and then at higher pH values the current decreases abruptly (16). This supports the anticipated performance of proton-dependent method with irreversible chemical reaction. The complete work was carried out with pH of 7.0.

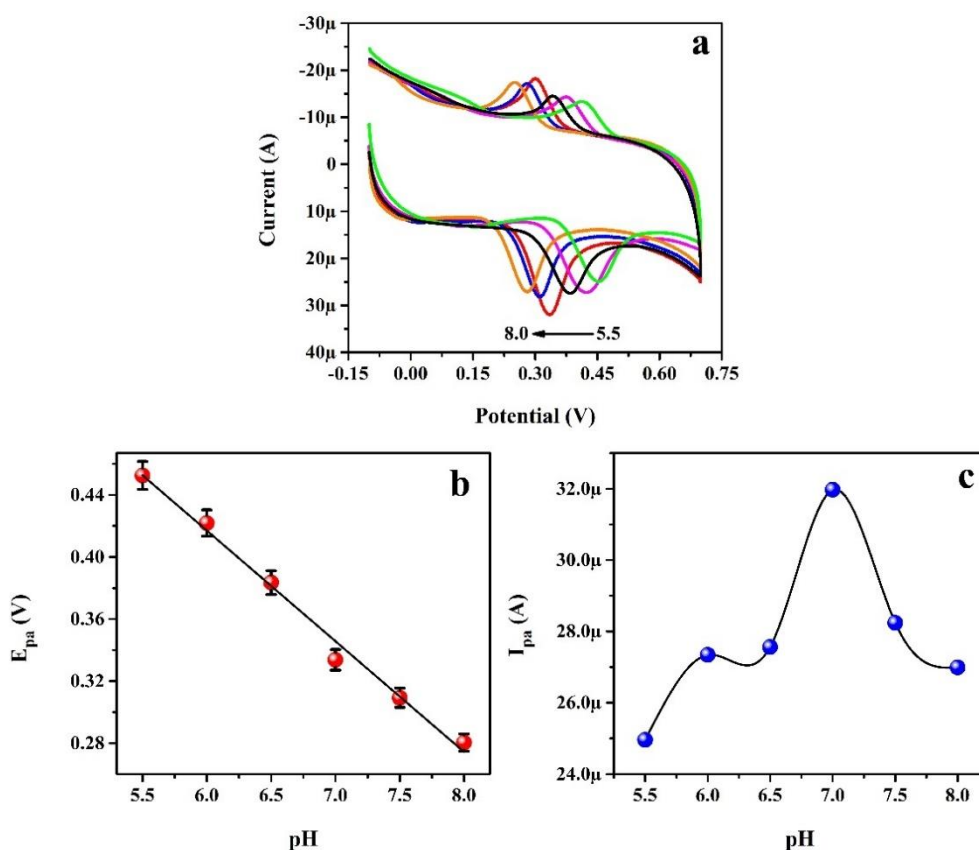


**Figure 6.** (a) CVs of 0.1 mM PRT in 0.2 M PBS of different pH from 5.5 to 8.5 on PAMCPS at the scan rate of 0.1 V/s. (b) Plot of  $E_{pa}$  vs pH. (c) Plot of  $I_{pa}$  vs pH.

### 3.2 Simultaneous determination of PRT in presence of CN

The instantaneous inspection of PRT with CN in 0.10 M PBS with pH of 6.5 on BCPS and PAMCPS was completed via the operation of CV at 0.1 V/s scan rate (Fig. 7). At BCPS, PRT and CN molecules shows weak electrochemical activity with lesser sensitive oxidation and reduction peak

currents with higher peak potentials. But at PAMCPS, PRT and CN displays distinguished electrochemical oxidation and reduction with superior redox peak currents and decreased redox potentials. This data discloses that, PAMCPS is superior for the examination of PRT in the incidence of CN with higher electrocatalytic accomplishment and fast electron transportation rate than BCPS.

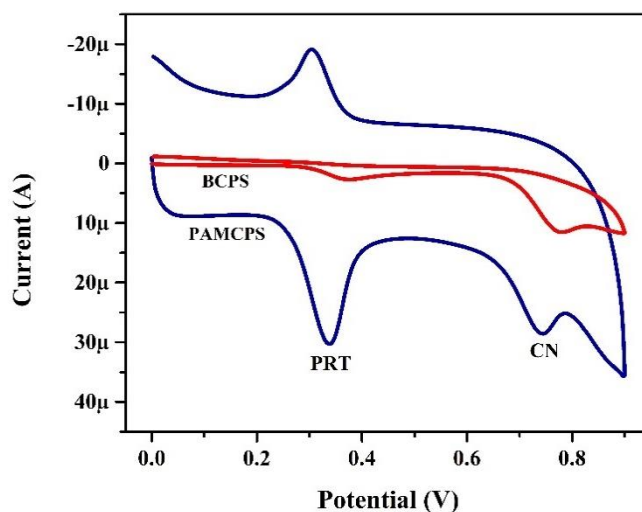


**Figure 7.** (a) CVs of 0.1 mM PRT and 1.0 mM CN in 0.2 M PBS of 7.0 pH on PAMCPS at the scan rate of 0.1 V/s.

### 3.2 Analytical curve application

The differential pulse voltammograms (DPVs) for PAMCPS (Fig. 8a) were achieved with successive adding of PRT at the enhanced experimental conditions. The analytical curve revealed in Fig. 8b, showed an agreeable linear range from 10.0  $\mu\text{M}$  – 105.0  $\mu\text{M}$  and the regression equivalence is as follows,

$$I_{pa} = 1.468 \times 10^{-5} + 0.295 [\text{HCQ}] (\text{M}) \quad (R = 0.999) \quad (\text{Eqn. 4}),$$

The DL and DQ are calculated using the the slope pf calibration curve and the following relations,

$$\text{DL} = 3.0 \text{ M/B} \quad (\text{Eqn. 5})$$

$$\text{DQ} = 10.0 \text{ M/B} \quad (\text{Eqn. 6})$$

where, M is the standard deviation of the blank and B is the slop of analytical curve, The calculated values of DL and DQ were attained to be 53.37 nM and 117.93 nM, which are values as assorted to some previously reported PRT sensors (Table 1) [41-47].

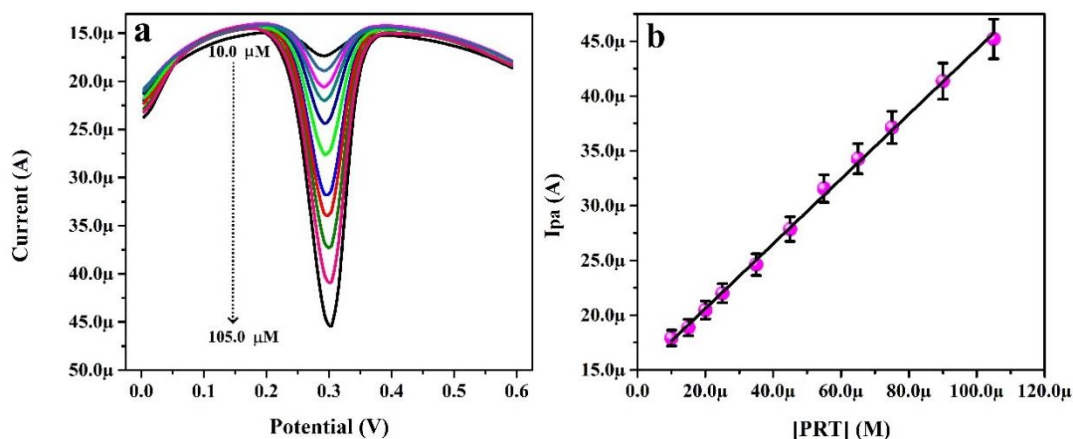


**Figure 8.** (a) DPVs of PRT having different concentration ranging from 10.0  $\mu\text{M}$  – 105.0  $\mu\text{M}$  in 0.2 M PBS of 7.0 pH on PAMCPS . (b) Plot of  $I_{pa}$  vs [PRT]

**Table 1.** Comparison data of current PRT sensor with previously reported PRT sensors

Electrode	Linear range	LOD	Reference
Multi walled carbon nanotubes-Nafion/glassy carbon electrode	2.0 $\mu\text{M}$ – 180 $\mu\text{M}$	0.5 $\mu\text{M}$	41
MoS <sub>2</sub> /TiO <sub>2</sub> NC modified GCE electrode	0.5 $\mu\text{M}$ – 750 $\mu\text{M}$	0.01 $\mu\text{M}$	42
Carbon paste electrode modified by coffee husks	6.6 $\mu\text{M}$ – 500 $\mu\text{M}$	0.66 $\mu\text{M}$	43
Pt/CeO <sub>2</sub> /Cu <sub>2</sub> O nanocomposites	0.5 $\mu\text{M}$ – 100 $\mu\text{M}$	0.091 $\mu\text{M}$	44
glassy carbon electrode (GCE) using multiwalled carbon nanotube (MWCNT) decorated with bismuth oxide	0.02 $\mu\text{M}$ – 28 $\mu\text{M}$	0.0052 $\mu\text{M}$	45
Hollow N,S-doped Carbon@Pd Nanorods	33 nM - 120 $\mu\text{M}$	11.0 nM	46
Cobalt ferrite modified graphite paste electrode	3–200	250 $\mu\text{M}$	47
Manganese-ferrite modified graphite paste electrode	3–160	300 $\mu\text{M}$	
PAMCPS	10.0 $\mu\text{M}$ – 105.0 $\mu\text{M}$	53.37 nM	Present work

### 3.2 Real sample analysis

To exhibit the relevance of the proposed strategy and electrode for the detection of PRT real sample (tablet) was analyzed. PRT content of the sample was subjected to DPV at PAMCPS using standard addition method. The results are collected in Table 2. It shows that, the good recuperation of PRT was observed in the range of 96.96% to 99.82%. This suggests that, the projected method is relevant to the examination of medicinal samples in presence of different matrices.

**Table 2.** Recovery of PRT in PRT medicinal sample.

Sample	Added in $\mu\text{M}$	Found in $\mu\text{M}$	Recovery in %
PRT tablet sample	25.00	24.24	96.96
	35.00	34.58	98.80
	45.00	44.91	99.82

### 3.2 Reproducibility, repeatability and stability

The PAMCPS reproducibility was measured by documenting five CV cycles for PRT in PBS at five different PAMCPSs. Here, the equipped PAMCPS provides the relative standard deviation (RSD) of 3.4%, suggesting an acceptable reproducibility of PAMCPS. The PAMCPS repeatability was measured by recording five CV cycles for PRT (changed at the end of each cycle) in PBS at fixed PAMCPS. Here, the equipped PAMCPS delivers the RSD of 3.03%, signifying an adequate repeatability of PAMCPS. The PAMCPS stability for PRT in PBS was inspected through CV method through cycling 30 CV cycles. The obtained value of percentage degradation shows 91.20% the regaining of initial current, which suggests acceptable PAMCPS stability.

## 4. CONCLUSIONS

The present attempt proposes an approachable and simple PAMCPS for the inspection of PRT in presence of CN thru CV technique, which displays fine conductivity, selectivity and sensitivity. The analytical procedure has been exclusively validated through fine linear association, accuracy, repeatability and reproducibility due to the enhancement of the electron transfer rate with a greater active surface area and active sites of PAMCPS. This examination gives a robust, modest and detailed analysis of PRT and its implication in PRT medicinal sample. Moreover, PAMCPS presents an appropriate and appropriate performance for the simultaneous detection of PRT in the presence of CN.

### ACKNOWLEDGEMENTS

The authors acknowledge the Deanship of Scientific Research at King Faisal University, Kingdom of Saudi Arabia for their financial support under Nasher Track (Grant No. 206033) and their encouragement.

### References

1. M.H. Pournaghi-Azar, H. J. Dastangoo. *J. Electroanal. Chem.*, 567 (2004) 211.
2. S.M. Chen, S.H. Hsueh. *J. Electrochem. Soc.*, 150 (2003) 175.
3. K. Kalcher, J.M. Kauffmann, J. Wang, I. Svancara, K. Vytras, C. Neuhold, Z. Yang. *Electroanalysis*, 7 (1995) 5.
4. I. Svancara, K. Vytras, J. Zima, J. Barek. *Crit. Rev. Anal. Chem.*, 31 (2001) 311.
5. A. Yigit, Y. Yardim, M. Celebi, A. Levent, Z. Senturk. *Talanta*, 158 (2016) 21.

6. C. Celma, J.A. Allue, J. Prunonosa, C. Peraire, R. Obach. *J. Chromatogr. A*, 870 (2000) 77.
7. Q.Y. Tan, R.H. Zhu, H.D. Li, F. Wang, M. Yan, L.B. Dai. *J. Chromatogr. B*, 162 (2012) 893.
8. L.M. Madikizela, N.T. Tavengwa, L. Chimuka. *J. Pharm. Biomed. Anal.*, 147 (2018) 624.
9. S.L. Zhao, W.L. Bai, H.Y. Yuan, D. Xiao. *Anal. Chim. Acta*, 559 (2006) 195.
10. T. Belal, T. Awad, C.R. Clark. *J. Chromatogr. Sci.*, 47 (2009) 849.
11. V.D. Hoang, D.T.H. Ly, N.H. Tho, H.M.T. Nguyen. *Sci. World J.*, 2014 (2014) 1.
12. M. Knochen, J. Giglio, B.F. Reis. *J. Pharm. Biomed. Anal.*, 33 (2003) 191.
13. J.G. Manjunatha, M. Deraman, N.H. Basri, I.A. Talib. *Adv Mat Res.*, 895 (2014) 447.
14. Z.I. Zarandy, M. Dehestani. *Chemistryselect.*, 4 (2019) 7866.
15. A.B. Monnappa, J.G. Manjunatha, A.S. Bhatt, H. Nagarajappa. *J. Sci. Adv. Mater. Devices*, 6 (2021) 415.
16. J.G. Manjunatha, C. Raril, N. Hareesha, M.M. Charithra, P.A. Pushpanjali, G. Tigari, D.K. Ravishankar, S.C. Mallappaji, J. Gowda. *Open Chem. Eng. J.*, 14 (2020) 90.
17. S. Bahmanzadeh, M. Noroozifar. *J. Electroanal. Chem.*, 809 (2018) 153.
18. N. Hareesha, J.G. Manjunatha, B.M. Amrutha, P.M. Pushpanjali, M.M. Charithra, N. Prinith Subbaiah. *J. Electron. Mater.*, 50 (2021) 1230.
19. N. Hareesha, J.G. Manjunatha. *Sci Rep.*, 11 (2021) 12797.
20. P.A. Pushpanjali, J.G. Manjunatha, H. Nagarajappa, Edwin S D' Souza, M.M. Charithra, N.S. Prinith. *Surf. Interfaces*, 24 (2021) 101154.
21. M. Mazloun-Ardakani, H. Beitollahi, M.K. Amini, B.F. Mirjalili and F. Mirkhalaf. *J. Electroanal. Chem.*, 651 (2011) 243.
22. P.A. Pushpanjali, J.G. Manjunatha, H. Nagarajappa, B.M. Amrutha, C. Raril, Zeid A. ALOthman, Amer M. Alanazi, A. Pandith. *Mater. Chem. Phys.*, 276 (2022) 125392.
23. Hossein Bahramipur Fahimeh, Jalali Fahimeh Jalali. *Afr. J. Pharm. Pharmacol.*, 6 (2012) 1298.
24. T. Eren, N. Atar, M. Lütüfi Yola, H. Karimi-Maleh. *Food Chem.*, 185 (2015) 430.
25. P.M. Pushpanjali, J.G. Manjunatha, B.M. Amrutha, H. Nagarajappa. *Mater. Res. Innov.*, (2020) 412.
26. N.S. Prinith, J.G. Manjunatha, H. Nagarajappa. *J Iran Chem Soc.*, 18 (2021) 3493.
27. A.M. Fekry, S. Gawad, R. Tammam, M. Zayed. *Measurement.*, 163 (2020) 107958.
28. P.M. Pushpanjali, J.G. Manjunatha, H. Nagarajappa. *J. Electrochem. Sci. Eng.*, 11 (2021) 161.
29. G. Tigari, J.G. Manjunatha, H. Nagarajappa, N.S. Prinith. *J. Electrochem. Sci. Eng.* (2021). DOI: <https://doi.org/10.5599/jese.1094>.
30. R.A. Ahmed, A.M. Fekry, R.A. Farghali. *Appl. Surf. Sci.* 285 (2013) 309.
31. N. Hareesha, J.G. Manjunatha, B.M. Amrutha, N. Sreeharsha, S.M. Basheeruddin, Md. Asdaq, K. Anwer. *Colloids Surf. A Physicochem. Eng.*, 626 (2021) 127042.
32. C. Karaman, O. Karaman, N. Atar and M. Lütüfi Yola. *Microchim. Acta.* 188 (2021) 182.
33. D.N. Varun, J.G. Manjunatha, N. Hareesha, et al. *Monatsh Chem.*, 152 (2021) 1183.
34. F. Tahernejad-Javazmi, M. Shabani-Nooshabadi, H. Karimi-Maleh. *Talanta.* 176 (2018) 208.
35. C. Raril, J.G. Manjunatha. *J Anal Sci Technol.*, 11 (2020) 3.
36. N. Hareesha, J.G. Manjunatha. *Mater. Res. Innov.*, 24 (2020) 349.
37. G. Tigari, J.G. Manjunatha. *J. Anal. Test.*, 3 (2020) 331.
38. C. Raril, J.G. Manjunatha, G. Tigari. *Instrum Sci Technol.*, 48 (2020) 561.
39. J. Jun, L. Lulu, L. Guoping, W. Dan, Z. Yan, C. Lijuan, Z. Junwei. *Inorg. Chem.*, 59 (2020) 15355.
40. M.M. Charithra, J.G. Manjunatha, *Chem. Data Coll.*, 33 (2021) 100718.
41. Zai-Yu Li, Dan-Yang Gao, Zhi-Yong Wu and Shuang Zhao, *RSC Adv.*, 10 (2020) 14218.
42. K. Nishant, S.B. M. Akhshay Boris, S. Suman, K. Christine. *Sens. Bio-Sens. Res.*, 24 (2019) 100288.
43. S.F. Mbokou, M. Ponti, J.P. Bouchara, et al., *Int. J. Electrochem.* 2016 (2016) 10.
44. R.R. Athimotlu, and Sebastian, C.P. *ACS Appl. Nano Mater.*, 1 (2018) 5148.
45. A.T. Chipeture, D. Apath, M. Moyo, *J Anal Sci Technol.*, 10 (2019) 22.

46. W. Linyu, Y. Yuxi, L. Huihui, W. Na, P. Xia, W. Li, S. Yonghai. *J. Hazard. Mater.*, 409 (2020) 124528.
47. K. Yogendra, P. Panchanan, K.D. Dipak. *Heliyon*, 5 (2019) e02031.

© 2022 The Authors. Published by ESG ([www.electrochemsci.org](http://www.electrochemsci.org)). This article is an open access article distributed under the terms and conditions of the Creative Commons Attribution license (<http://creativecommons.org/licenses/by/4.0/>).